ISSN 0010-9525, Cosmic Research, 2017, Vol. 55, No. 2, pp. 79–87. © Pleiades Publishing, Ltd., 2017.
Original Russian Text © M.I. Panasyuk, M.V. Podzolko, A.S. Kovtyukh, I.A. Brilkov, N.A. Vlasova, V.V. Kalegaev, V.I. Osedlo, V.I. Tulupov, I.V. Yashin, 2017, published in Kosmicheskie Issledovaniya, 2017, Vol. 55, No. 2, pp. 85–93.

Optimization of Measurements of the Earth's Radiation Belt Particle Fluxes

M. I. Panasyuk, M. V. Podzolko, A. S. Kovtyukh, I. A. Brilkov, N. A. Vlasova, V. V. Kalegaev, V. I. Osedlo, V. I. Tulupov*, and I. V. Yashin

Skobeltsyn Institute of Nuclear Physics, Moscow State University, Moscow, Russia

**e-mail: ikt0840@mail.ru*

Received June 3, 2015

Abstract—The Earth's radiation belts discovered at the end of the 1950s have great scientific and practical interest. Their main characteristics in magnetically quiet periods are well known. However, the dynamics of the Earth's radiation belts during magnetic storms and substorms, particularly the dynamics of relativistic electrons of the outer belt, when Earth's radiation belt particle fluxes undergo significant time variations, is studied insufficiently. At present, principally new experiments have been performed and planned with the intention to better study the dynamics of the Earth's radiation belts and to operationally control the space-energy distributions of the Earth's radiation belt particle fluxes. In this paper, for spacecraft designed to measure the fluxes of electrons and protons of the Earth's radiation belts at altitudes of 0.5–10000 km, the optimal versions for detector orientation and orbital parameters have been considered and selected.

DOI: 10.1134/S0010952516060071

INTRODUCTION

At present, to estimate the radiation conditions in satellite orbits, the averaged empirical models of the space-energy distributions of the particle fluxes of the Earth's radiation belts (ERBs) are used, for example, American *AE*8 [1] and *AP*8 [2] and Russian [3, 4]. In these models, the spatial distributions of ERB particles are symmetric over MLT and stationary, solar-cyclic ERB variations are only reflected for periods of the minimum and maximum solar cycle.

However, during the geomagnetic storms, and at large L – during the qiuiet periods as well, the distributions of the ERB particle fluxes are asymmetric over MLT. During storms and substorms space-energy distributions of ERB particles vary greatly and, during strong geomagnetic storms, electron ERBs can completely reform (see, e.g., [5]). This can lead to significant errors when calculating the radiation doses in satellite orbits, but is not adequately reflected in the current empirical ERB models.

Let us consider the main characteristics and the dynamics of ERBs in detail.

SPACE-ENERGY DISTRIBUTIONS AND VARIATIONS OF THE EARTH'S RADIATION BELT PARTICLE FLUXES

ERBs fill the entire region of geomagnetic trap and consist of mainly electrons and protons with energies from ~100 keV to several hundreds of MeV. Heavier charged particles contribute slightly (several percent) to the total number of ERB particles (~10^{29}–10^{30}). ERB electrons and protons are major contributors in the radiation doses on satellites.

Due to the conservation of the adiabatic invariants of motion, particles injected into a point of geomagnetic trap gradually occupy a closed toroidal surface, a drift shell. The meridional section of the shell coincides with one of the magnetic lines and the equatorial section with one of the magnetic isolines. Therefore, the experimental distributions of ERB particles are most simply systematized in the McIlwain coordinates $\{L, B\}$: L is the drift shell parameter and B is the local induction of magnetic field. For the dipole field L is the distance from the top of field lines to the Earth's center in terms of Earth's radii.

In the region of the dipole magnetic field the drift shells are symmetric over longitude and local time (surface of revolution), and in the outer part of geomagnetic trap (during quiet periods at $L > 5$), these shells are asymmetric and depend on the equatorial particle pitch angle α_0 (the angle between vectors of the magnetic field and the particle velocity at the top of the magnetic tube), i.e., in this region, the drift shells split [6].

In the night hemisphere, the value $B(\lambda)$ for this field line is minimum at the geomagnetic latitude $\lambda = 0$, and in the near-noon sector at $L > 9$, this dependence has local maximum at $\lambda = 0$ and local minimum at $\lambda \sim 40$–$50°$ (the result of the magnetospheric compression by the solar wind). During the drift of trapped particles in this region, the second invariant is violated and the belts are split into two branches (in the northern and southern hemispheres), the effect of branching of the drift shells [7].

In contrast of protons, electrons form in geomagnetic trap two belts: inner and outer. In quiet periods, electron belts are separated by a deep gap at $L = 2.2$–3.5 (depending on the particle energy). The gap depth increases with the increase of the energy of electrons. In comparison with the proton belt, the maximum of the outer belt of electrons of the same energies is located at larger L. With increasing the solar activity the maximum of the outer belt of electrons with $E >$ 0.1 MeV is shifted to the Earth from $L_m \sim 5$ to ~ 3.7 [8]. After every storm, a new belt of energetic electrons is formed and, in this case, L_m is the smaller the greater $\max|Dst|$ during the storm [8].

Compared with protons, ERB electrons have much shorter lifetimes and, for a sufficiently long duration of the quiet period, almost all electrons with $E > 0.5$ MeV can disappear from the outer belt. Therefore, the outer electron belt is much more sensitive to the geomagnetic activity than the proton belt. In the geostationary orbit (GSO), storm/substorm bursts of the relativistic electron fluxes are often observed by an order of magnitude or more. The possibility of these bursts is maximum in periods of minimum solar activity. Thus, the integral annual flux of electrons with $E > 3$ MeV in GSO for the year of the minimum solar activity (1984) was greater than for the year of maximum (1979) by a factor of seven [9].

The electron fluxes of the outer belt undergo also 27-day variations [10] and semiannual (seasonal) variations that correlate with the average velocity of the solar wind [11].

During geomagnetic storms, ERB proton fluxes are weakened and then restored. On the other hand, the outer belt of nonrelativistic electrons becomes stronger in the main phase of the storm is moved to the Earth and the gap between the belts is partially or fully (during fairly strong storms) filled. At the end of the storm, the radial profiles of the fluxes of nonrelativistic electrons, as well as protons, are fully restored.

However, during strong ($Dst < -100$ nT) storms, the dynamics of the relativistic electron belt is principally different; in the main phase, the old belt of relativistic electrons is significantly weakened or even disappears and, in the phase of the storm restoration, a new belt of relativistic electrons is formed that is more intensive and located closer to the Earth. Immediately after the formation, the maximum of this belt is located at $L_m \sim 2.5$–5.5, in this case, L_m is the smaller the greater is $S \equiv \max|Dst|$ of the storm [8]. The location of the maximum of this belt over L does not depend of the energy of relativistic electrons [12].

Decreasing the relativistic electron fluxes in the main phase of the strong storm reaches 1–2 orders of magnitude. New belt of relativistic electrons is formed in the beginning of the phase of the storm restoration and next 1–2 weeks gradually increases and shifts to the Earth. At high altitudes, $L_m \approx 12.8S^{-0.25}$ [13]. At low altitudes, this dependence is stronger, i.e., $L_m \approx 12.8S^{-0.41}$ [14], which indicates the considerable deviation of the geomagnetic field from the dipole configuration, even in the depth of ERB during strong storms.

This dynamics of the outer belt of relativistic electrons is characteristic of strong storms. For weak and moderate storms, the dynamics of this belt is less predictable. Thus, in approximately half of the 276 moderate and strong storms in 1989–2000 considered in [15], the relativistic electron fluxes to the end of the storm increased, they were reduced in one-fourth of events, and nearly unchanged (restored to initial levels) in 1/4 of storms.

As a rule, the fluxes of relativistic electrons of the outer belt are generated in periods, when strong geomagnetic disturbances ($Dst < -100$ nT) are combined with the high velocity of the solar wind in the vicinity of the Earth [12, 15, 16] and the substorm activity in the phase of the storm restoration [13]. A new belt of relativistic electrons begins to form through approximately 2 days after a sharp increase in the velocity of the solar wind (up to the value of >450 km/s) or coming dense clusters of solar plasma (coronal mass ejections) to the geomagnetosheric boundaries; in the first case, the incipient new belt is very narrow and, in the second case, it is much wider [16].

In the modern physics of ERBs, the problem of the dynamics of the relativistic electron belt holds a special place. They are also making considerable and almost unpredictable contribution in the radiation dose in the satellite orbits.

For each ERB component, the particle flux is a function of many variables. When considering the dependence of the fluxes from one of these variables, the following distributions are considered: *the radial dependence*, i.e., the dependence on L; *the diurnal dependence*, i.e., the dependence on LT or MLT; *the energy spectra*, i.e., the dependence on E; *the pitch angle distributions* (PAD), i.e., the dependence on equatorial α_0 or local pitch angle α; and *the altitude dependence*, i.e., the dependence on B/B_0. These distributions vary during the geomagnetic activity and depend on the phase of the solar cycle, conditions in the interplanetary space, and other factors.

The radial dependence of the ERB particle fluxes is considered above. The diurnal dependence of the ERB particle fluxes manifests well in the geostationary orbit and is closely associated with the asymmetry of the magnetosphere (see, e.g., [17]). Let us briefly consider the energy spectra, PADs, and altitude dependences of ERB protons and electrons.

At fairly high energies, the ERB proton spectra have the power form $j(E) \propto E^{-\gamma}$ at $E > (35 \pm 11)L^{-3}$ MeV, where $\gamma = 4.25 \pm 0.75$ at $L > 3.5$; at lower energies, the ERB proton spectra are flattened and the local maximum is planned at $E_m = (17 \pm 3)L^{-3}$ MeV [18, 19]. With an increase in the mirror ratio B/B_0 (decrease of α_0 of particles) at the given L the ERB proton spectra are softened, and the maximum in the spectra is shifted to lower energies and narrowed (see, e.g., [20]).

In the quiet periods, the energy spectra of nonrelativistic electrons of the outer belt can be approximated by the Maxwell distribution with temperature $T = (6 \pm 1)\ (6.6/L)^3$ keV [21]. In the inner belt, the spectra of relativistic electrons can be approximated by an exponential function with $E_0 \sim 300$ keV and higher [22]. In the gap between the belts in the electron spectra, the deep dip is formed at ~0.5 MeV, which is filled during storms.

Typical PADs of ERB protons have the maximum at $\alpha_0 = 90°$ ("normal"). These PADs correspond to the altitude dependence decaying to the Earth. The average parameter of the PAD anisotropy of ERB protons increases with decreasing L and with increasing particle energy (see, e.g., [23]). At larger L (in the region of splitting and branching drift shells), PADs of ERB protons can have the butterfly form (see, e.g., [24]).

PADs of ERB electrons are very diverse in form and vary greatly during geomagnetic disturbances. In the outer belt, on average, these distributions are more isotropic than in the inner belt and vary much more. At $L < 5$, they usually have a normal form and the average anisotropy parameter increases with decreasing of L, achieving $A \approx 6$ and more at $L \approx 1.6$ [25]. At $L > 5$–6 (in the region of splitting and branching drift shells), PADs of ERB electrons have diverse, often normal or butterfly form [26].

Hereafter, great attention will be given to the altitude dependence of the ERB particle fluxes. Therefore, here, we consider this question in detail.

Using the Liouville theorem, the altitude dependence of the ERB particle fluxes is unambiguously associated with particle PADs. When applied to ERBs, this theorem is strictly satisfied for stationary conditions when the magnetic field does not change with time, there are no electric fields, and particles do not lose energy by interaction with other particles or waves. It is also satisfied for quasi-stationary conditions when the magnetic field is changed, but rather slow and first two adiabatic invariants of the ERB particle motion are preserved; there are electric fields, waves, and other particles, but their action on ERB particles in the period of oscillations of the latter between mirror points can be neglected. Under the conditions of ERBs, indicated conditions of quasi-steady state are almost always satisfied and can only be violated during very strong geomagnetic disturbances.

According to this theorem, at each point of a given magnetic tube for particles with the same energy and α_0, the value of the ERB particle flux (differential j or integral J) is identical. In this case, it is necessary to take into account that, during oscillations, the ERB particle energy and their α_0 are preserved, and the magnetic field B and local particle pitch angle α increase with particle approaching to the Earth (to mirror point) according to the law derived from the conservation of the first motion invariant: $\sin\alpha = \sqrt{B/B_0}\sin\alpha_0$, where $B(L, h)$ is local magnetic induction and B_0 is its induction at the vertex of this tube (in the equatorial plane).

For practical purposes, in wide intervals of pitch angles, PADs of ERB particles are well approximated by the function $j \propto \sin^A\alpha$, where $A(L, E)$ is the anisotropy parameter of this PAD. For these PADs, according to the Liouville theorem, the altitude dependence of the fluxes for particles with the given energy at given L has the form $j \propto (B/B_0)^{-A/2}$.

In different altitude intervals (intervals of B/B_0) the slope of altitude dependence (the $A/2$ index) can be different. Therefore, the altitude dependence of the ERB particle fluxes can be approximated by a power function with different exponents in different parts of this dependence or with some unified function. Because a break occurs in the altitude dependence (sharp exponential steepening) at large values B/B_0, we can use, e.g., the following dependence as a unified approximation function:

$$j \propto (B/B_0)^{-n}\exp\left(-a(B/B_0)^m\right),$$

where a, n, and m are positive parameters, which differ for different L and particle energies.

Fundamentals of the ERB physics are presented in the monographs [6, 27–30]. A modern systematic presentation of the ERB physics, main experimental results on the ERB structure and dynamics, the mechanisms of their formation, and the mechanisms of acceleration and particle losses can be found in the review [31].

MEASUREMENTS ON MULTIDISCIPLINARY RESEARCH SATELLITES

A typical instrument construction for measuring the energy spectra of ERB electrons and protons is assembly as a telescope, including several semiconductor and scintillation detectors of different thickness located coaxially one under the other. Similar telescopes were installed, e.g., on the *Electro* spacecraft [32]. Charged particles that pass through the input telescope window and enter into a detector release energy in it, which is transformed into an electrical impulse with intensity proportional to the energy released. The assembly of several detectors and electronic logic schemes that operate according to the

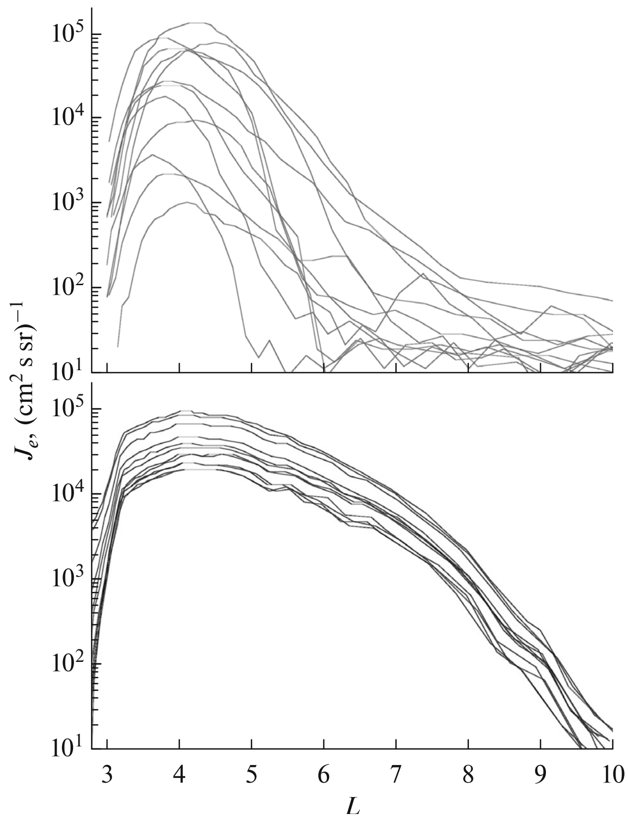

Fig. 1. L-profiles of the fluxes of electrons with $E = 0.3$–0.6 MeV in the outer belt obtained on the *Universitetsky-Tatiana* spacecraft (at the top) and calculated according to the *AE*8 model (at the bottom).

principle of the coincidence–anticoincidence of impulses in different detectors allows to determine the particle type (electrons, protons) and exclude lateral particle passage (through the telescope body). The angle of the telescope aperture should be limited by the value ~60°, because in the instrument with wider field of view it is impossible practically to separate electrons and protons.

In the simplest version, on the multi-disciplinary research satellites one spectrometer for measuring the ERB particle fluxes can be installed. In this case, it is desirable to orient the telescope in such manner that when passing ERB it recorded particles with local pitch angles of ~90°, for which the particle fluxes are maximum.

For example, we consider a low-orbit satellite that has, in particular, instruments for studying the Earth's surface or atmosphere. One of the axes of these satellites is directed to the Earth's (to the nadir), while, in the case of three-axis orientation, the other is directed along the satellite's velocity vector. On these satellites, the spectrometer of energetic particles is usually oriented to the nadir, e.g., on the *Universitetsky-Tatiana* and *Meteor-M* spacecrafts. However, this detector orientation is nonoptimal, especially when measuring the particle fluxes of the outer radiation belt. L-profiles of the fluxes of electrons with $E = 0.3$–0.6 MeV in the outer belt obtained on the *Universitetsky-Tatiana* spacecraft during several orbits around the Earth in the magnetically quiet period (the end of April 2006) are presented at the top of Fig. 1. The *Universitetsky-Tatiana* spacecraft was launched in January 2005 in orbit with an altitude of ~940 km and an inclination of ~83° [33]. For comparison, at the bottom of Fig. 1, we present L-profiles of corresponding electron fluxes calculated according the *AE*8 model (for recalculating the model values in the unidirectional flux, the multiplier 2π was used).

It can be seen from Fig. 1 that the fluxes measured on the *Universitetsky-Tatiana* spacecraft are, on average, lower than the model values and vary ten times more from the latter. Moreover, at $L > 6$–6.5, according to the data of the *Universitetsky-Tatiana* spacecraft, the fluxes decrease up to the background level of the detector count, whereas in the *AE*8 model, there are the fluxes at this altitude up to $L = 8$–9. The obtained result can be explained by the fact that the detector on the *Universitetsky-Tatiana* spacecraft was oriented to the Earth and at the latitudes of the outer belt detected particles with small pitch angles.

Figure 2 shows a map of distributions of the angles α between the detector axis and the magnetic field line for the telescope orientation to the Earth, as for the *Universitetsky-Tatiana* spacecraft, (at the top of Fig. 2) and perpendicularly to the orbit plane (at the bottom) for circular orbit with an altitude of 800 km and an inclination of 80°. The value of the angle α is shown by the arrow direction: the vertical corresponds to the angle of 90° and the horizontal to 0°.

It is seen from Fig. 2 that, for the detector orientation to the Earth, near the equator $\alpha \sim 90°$, but with increasing distance from the equator the value of the angle also decreases in the region of the outer belt at latitudes of 40°–80° depending on the longitude, $\alpha < 40°$. For the detector orientation perpendicular to the orbit plane $\alpha \sim 90°$ at almost all parts of the orbit (the minimum value $\alpha = 70°$). The orientation of the detector perpendicular to the orbit plane is optimal for measuring the ERB particle fluxes in the indicated orbit. This orientation is also achieved, e.g., in a solar-synchronous orbit with the orientation of the satellite to the Sun.

On multidisciplinary research satellites it is interesting to use an instrument for measuring charged particle fluxes that consists of several telescopes with different directions. This allows to perform measurements of the particle fluxes and their distributions over pitch angles with just small increase of mass and energy consumption.

For example, it can be proposed to use an instrument with four telescopes: the 1st telescope axis is directed to the Earth; the 2nd – perpendicularly to the orbit plane; the 3rd – along to the spacecraft velocity vector; the 4th – along the major diagonal of a cube

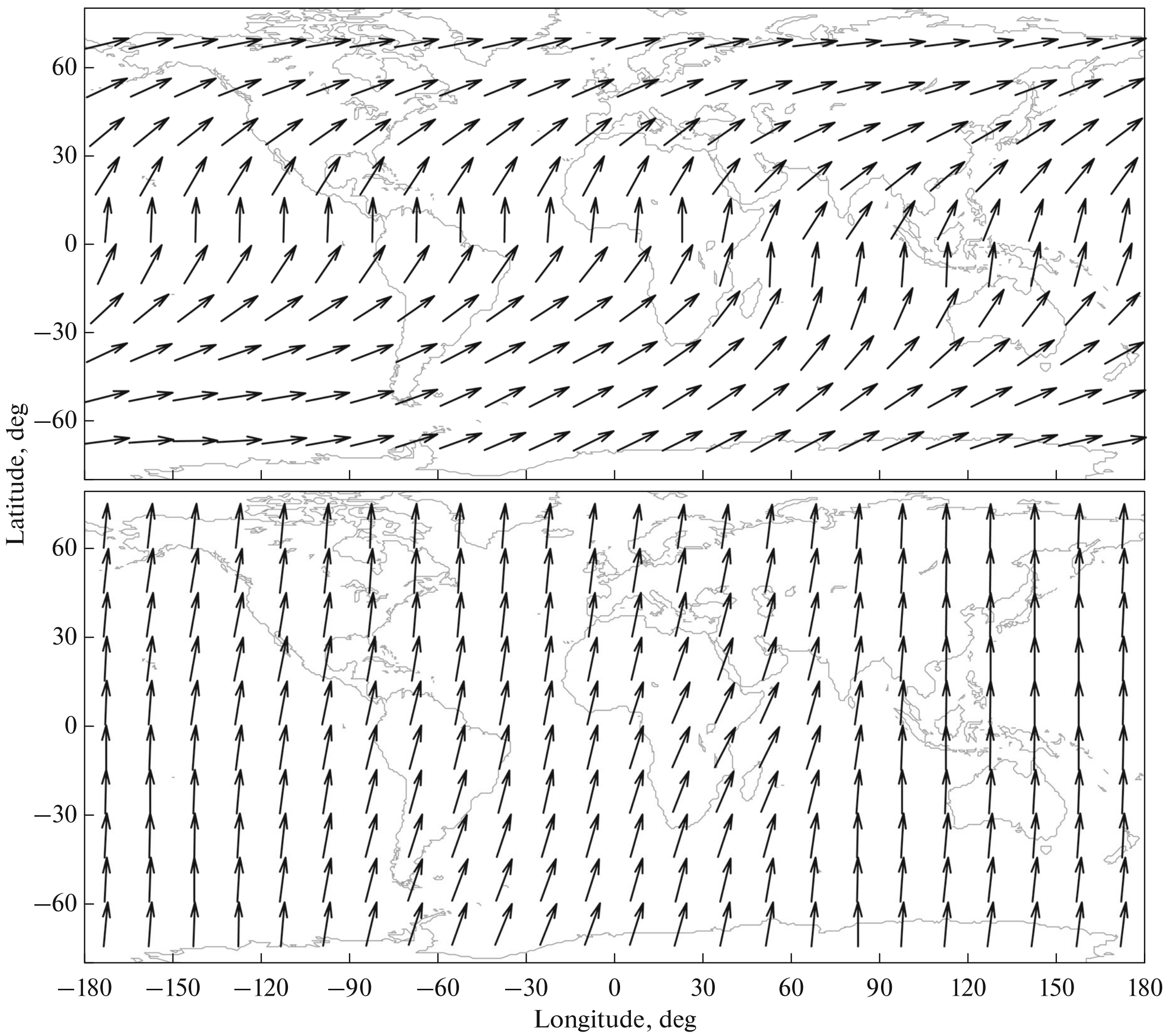

Fig. 2. Map of the distributions of the angles α between the detector axis and the magnetic field line (arrow direction) for the telescope orientation to the Earth (at the top) and perpendicular to the orbit plane (at the bottom) for circular orbit with an altitude of 800 km and an inclination of 80°.

constructed on the axes of first three. The distributions of the angles α between the axis of 3rd and 4th detectors and the magnetic field line for circular orbit with an altitude of 800 km and an inclination of 80° are shown in Fig. 3; and for the 1st and 2nd detectors – correspondingly in Fig. 2. Like Fig. 2, Fig. 3 was constructed for ascending parts of orbits. Similar figures are obtained for descending orbits.

It follows from Figs. 2 and 3 that, for this four-axis instrument, for ~90% of points of the orbit, we have no less than three pitch angles that differ by more than 10° and, for the remaining points, two different values of pitch angles. Thus, the proposed instrument with the given telescope orientation allows one to perform more detailed measurements of the particle fluxes at all orbit points. In principle, it can also be used on satellites with the orientation different from the three-axis "orbital" orientation.

SPECIALIZED SATELLITES FOR STUDYING THE RADIATION BELTS

The goal of specialized satellites for studying the radiation belts is to obtain a picture of the current space-energy distribution of the ERB particle fluxes in terms of L, B-coordinates. Measurements are needed, which allow one to construct the altitude dependences for the fluxes for different L-shells. This goal can be solved in several ways.

One of the ways is to measure the pitch angle distributions of the ERB particle fluxes near the plane of the magnetic equator in detail. Using these data in accordance with the Liouville theorem, the fluxes along entire drift shell of the particle motion can be calculated depending on the value of the local magnetic induction (see above). To cover the considerable range over L, it is necessary to select an elliptic orbit

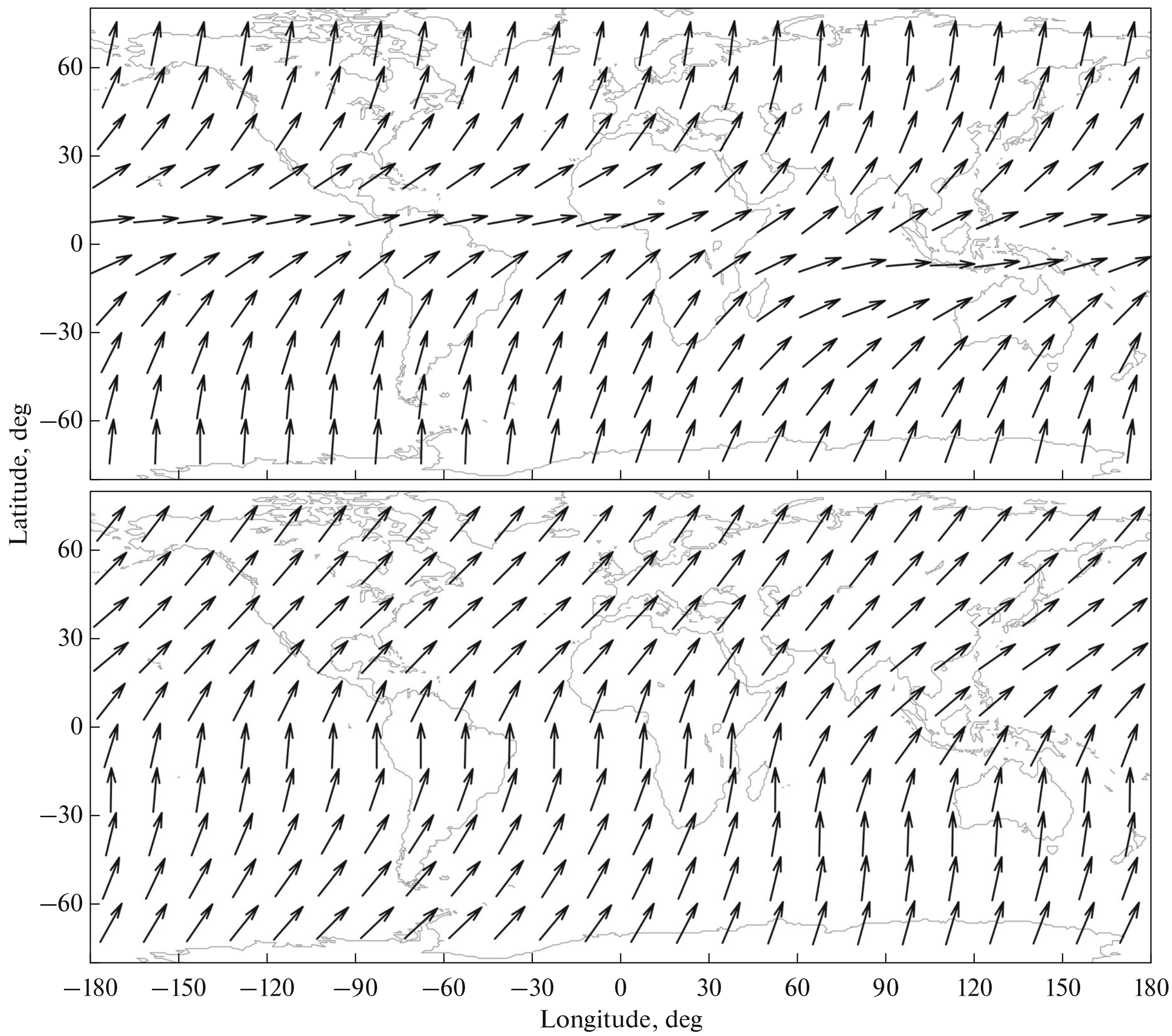

Fig. 3. Map of the distributions of the angles α between the detector axis and the magnetic field line (direction of the arrow) for telescope orientation along the spacecraft velocity vector (top) and along the major diagonal of a cube constructed on the axes of the first three telescopes (bottom) for circular orbit with an altitude of 800 km and an inclination of 80°.

with a perigee altitude of ~500–800 km and an apogee in the region of the geostationary orbit.

At present, in these orbits there are two *Van Allen Probes* satellites for studying ERBs [34]. These satellites include several detectors for measuring the fluxes of electrons with the energies from 20 keV to > 50 MeV and protons with the energies from 20 keV to > 200 MeV, as well as detectors of plasma, magnetic and electric fields, and waves. Detailed measurements of the pitch angle distribution of the particle fluxes are provided by rotating of the satellites with the period of ~11 s around the sunward axis. The resolution over pitch angles in the measurements of the ERB particle fluxes on the satellites is 11°–16°.

However, this procedure of measurements is associated with large cost of spacecraft launching into highly elliptic orbit. Also measurements at every given L are separated by long time intervals that, in many cases, do not allow one to trace the dynamics of the ERB particle fluxes during magnetic storms with sufficient detail.

It is possible to propose a different, less costly method based on measuring the omnidirectional flux of energetic particles at different points of the L-shell and constructing the flux altitude dependence according to these data. For this it is necessary to launch the satellite into such orbit, in which it will cross the drift shells at different altitudes. For example, the elliptic orbit with altitudes of a perigee of ~700 km and an apogee of 8000 km, an inclination of 63.4°, a perigee argument of 310° and the period of ~3 h. The projection of this orbit on the plane of geomagnetic meridian is shown in Fig. 4. As seen from Fig. 4, this orbit crosses the inner and outer belts at altitudes of 700–1500 and 4000–8000 km, where a principally different slope of the flux altitude dependence is observed. It is

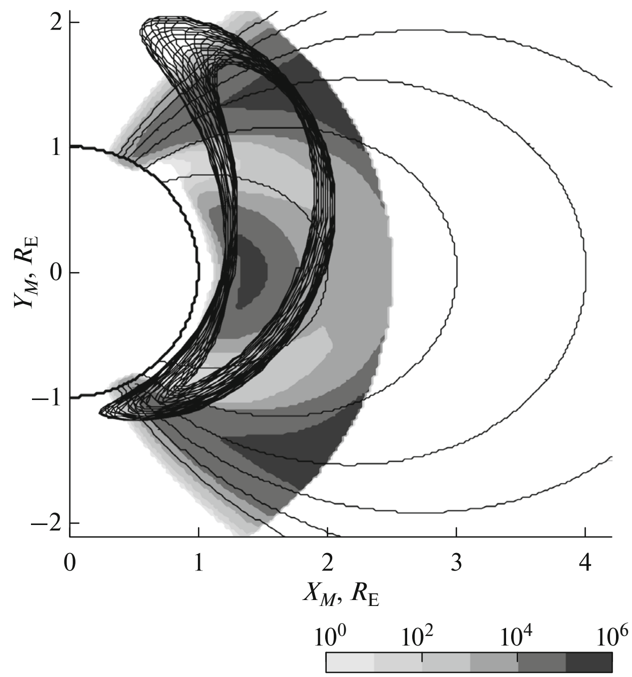

Fig. 4. Projection of elliptic orbit on the plane of the geomagnetic meridian. Lines denote the magnetic shells $L = 2$, 3, 4, 5, 6, and 7; shades of gray denote the values of the fluxes of electrons with $E > 2$ MeV according to the *AE*8 model.

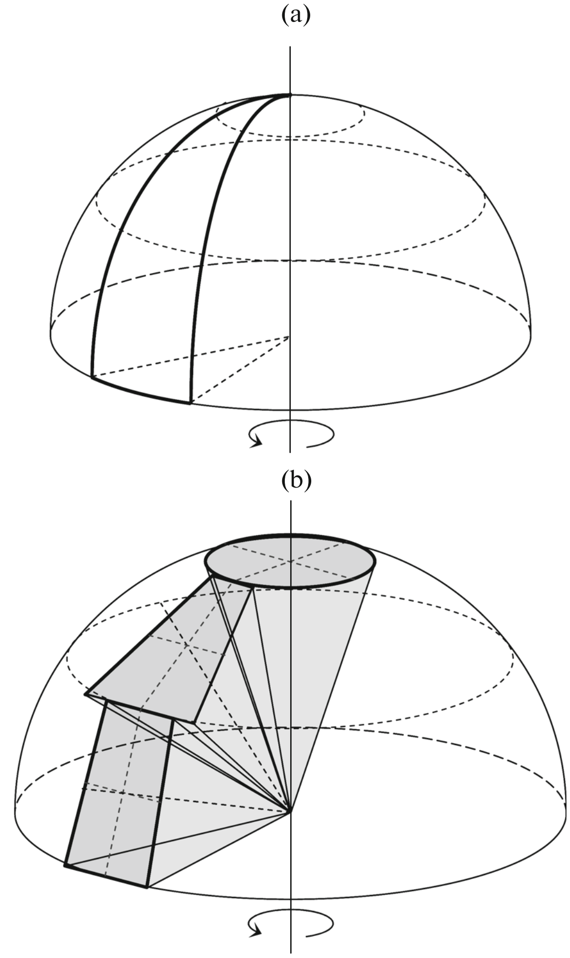

Fig. 5. Method of practically precise measurement of the omnidirectional particle fluxes: (a) field of view as rotating hemispherical sector; (b) configuration of three detectors.

important for an adequate approximation of the altitude dependence according to measurement data. The choice of the value of the orbit inclination of 63.4° is due to the fact that, for this inclination, the perigee argument does not change (under the influence of the second zonal harmonic of the Earth's gravitational field). According to our calculations, for the time resolution of 6 s at $L \leq 7$, the measurement resolution over L for this orbit $\Delta L \leq 0.2$; $\Delta L \leq 0.1$ at $L \leq 4.5$.

Some disadvantage of the proposed measurement ideology is the need to extrapolate the altitude dependence of the fluxes to altitudes of >8000 km, e.g., to orbits of the GPS and *GLONASS* satellite or geostationary satellites. However, in this region, the altitude dependence of the fluxes has a simple power law form and the extrapolation error should not be very large. We can slightly increase the apogee altitude of proposed orbit, for example, up to 10000 km; in this case, the extrapolation accuracy of the fluxes at L = 4–6 is improved by ~10%.

The alternative "intermediate" elliptic orbit may have: altitudes of a perigee and an apogee of 700 and 18000 km, an inclination of 32°, and initial value of a perigee argument of ~300°. The spacecraft in this orbit will observe ERB up to L = 7 and at higher L will be closer to the geomagnetic equator plane that will decrease the extrapolation errors. But for this orbit the perigee argument will vary with the speed of ~1.13 deg/day. At the worst value of the perigee argument equal to 0°, the ERB region crossed by the spacecraft is limited by L = 4.

In our ideology, it is necessary to obtain omnidirectional particle fluxes from measurements. However, as mentioned above, in a detector with a field of view of >60° the electron and proton fluxes are hardly separated. One solution is to use a configuration with several multidirectional telescopes (see the previous section) and then according to the data of their measurements to approximate the pitch angle particle distributions and calculate the omnidirectional fluxes.

Another way of the practically precise measurement of the omnidirectional fluxes of ERB particles can be carried out via three detectors that form the field of view in the sector of hemisphere (Fig. 5a). The rotation axis (vertical line) corresponds to the major satellite axis. If, in this case, the satellite is quickly rotated around its axis, this device provides an overview of the whole hemisphere.

For easier practical implementation of this idea the detector cross-sections were selected slightly diferent (see Fig. 5b). The aperture of the top (center) telescope has a conical form with a viewing angle of 36°, and the cross-sections of apertures for lateral telescopes have the form of trapezoids. The area of cross-sections of apertures for all detectors is the same.

Lateral detectors can be located on opposite sides from the rotation axis for centering the satellite mass. It can be used also five detectors by placing two pairs of lateral detectors symmetrically relative to the rotation axis. In this version, the hemisphere will be scanned for satellite half-turn around the axis, i.e., the spatial resolution of measurements will double. The period of the satellite rotation around its axis can be equal to several seconds. If multiple smaller time intervals of measuring the particle fluxes are used, data can be obtained on the pitch angular distributions of the fluxes; for this, a three-component magnetometer is necessary onboard the spacecraft.

The proposed orbits and measurement methods allow us to create a fairly simple and compact satellite for measuring the space-energy distributions of the ERB particle fluxes.

CONCLUSIONS

1. The space-energy distributions of the ERB particle fluxes are asymmetric over MLT and highly variable during geomagnetic storms and substorms, as well as in connection with the level and the type of solar activity. Therefore, the use of available averaged empirical ERB models is not sufficient to estimate the radiation conditions in the satellite orbits.

2. We analyzed different variants for installing detectors of energetic particles on satellites. We presented examples of fairly successful configurations with single or multiple telescopes, which allows us to measure the ERB particle fluxes at all orbit points in detail.

3. We analyzed different versions of orbits and measurement methods of specialized satellites for studying ERB. We proposed some versions of orbits and detector location, which allow one to create fairly simple and compact satellite systems for the operative monitoring of the space-energy distributions of the particle fluxes in the Earth's radiation belts.

ACKNOWLEDGMENTS

This study was prepared according to the results of applied scientific studies (unique identifier no. RFMEFI60414X0127) and supported by the Ministry of Education and Science of the Russian Federation.

REFERENCES

1. Vette, J.I., *The AE-8 Trapped Electron Model Environment*, Greenbelt, Maryland: National Space Science Data Center (NSSDC) World Data Center A for Rockets and Satellites (WDC-A-R&S), 1991.
2. Sawyer, D.M. and Vette, J.I., *AP-8 Trapped Proton Environment for Solar Maximum and Solar Minimum (Tech. Rep. 76–06)*, Greenbelt, Maryland: National Space Science Data Center (NSSDC) World Data Center A for Rockets and Satellites (WDC-A-R&S), 1979.
3. Getselev, I.V., Gusev, A.A., Darchieva, L.A., et al., *Model' prostranstvenno-energeticheskogo raspredeleniya potokov zakhvachennykh chastits (protonov i elektronov) v radiatsionnykh poyasakh Zemli* (Model of the Spatial and Energetic Distribution of Fluxes of Trapped Particles (Protons and Electrons) in the Earth's Radiation Belts), Moscow: MGU, 1991.
4. Getselev, I.V., Sosnovets, E.N., Kovtyukh, A.S., et al., An empirical model of the radiation belt of Helium nuclei, *Cosmic Res.*, 2005, vol. 43, no. 4, pp. 229–232.
5. Mullen, E.G., Gussenhoven, M.S., Ray, K., and Violet, M.A., A double-peaked inner radiation belt: Cause and effect as seen on CRRES, *IEEE Trans. Nucl. Sci.*, 1991, vol. 38, pp. 1713–1718.
6. Roederer, J.G., *Dynamics of Geomagnetically Trapped Radiation*, New York: Springer, 1970.
7. Shabanskii, V.P., *Yavleniya v okolozemnom prostranstve* (Phenomena in the Near-Erath Space), Moscow: Nauka, 1972.
8. Williams, D.J., Arens, J.F., and Lanzerotti, L.J., Observations of trapped electrons at low and high altitudes, *J. Geophys. Res.*, 1968, vol. 73, pp. 5673–5696. doi 10.1029/JA073i017p05673
9. Baker, D.N., Blake, J.B., Klebesadel, R.W., and Higbie, P.R., Highly relativistic electrons in the Earth's outer magnetosphere: 1. Lifetimes and temporal history 1979–1984, *J. Geophys. Res.*, 1986, vol. 91, pp. 4265–4276.
10. Williams, D.J., A 27-day periodicity in outer zone trapped electron intensities, *J. Geophys. Res.*, 1966, vol. 71, pp. 1815–1826.
11. Li, X., Baker, D.N., Kanekal, S.G., et al., Long-term measurements of radiation belts by SAMPEX and their variations, *Geophys. Res. Lett.*, 2001, vol. 28, pp. 3827–3830.
12. Gorchakov, E.V., Afanas'ev, V.G., Afanas'ev, K.G., et al., Study of fast charged particles with the help of a Cherenkov detector on the "Kosmos-900" artificial Earth satellite, *Izv. Vyssh. Uchebn. Zaved., Fiz.*, 1987, no. 10, pp. 69–74.
13. Tverskaya, L.V., The latitude position dependence of the relativistic electron maximum as a function of *Dst*, Adv. Space Res., 1996, vol. 18, no. 8, pp. 135–138.
14. Kovtyukh, A.S., Storm deviations of the geomagnetic trap core from dipole configuration deduced from data on relativistic electrons, *Cosmic Res.*, 2012, vol. 50, no. 3, pp. 226–232.
15. Reeves, G.D., McAdams, K.L., Friedel, R.H.W., and O'Brien, T.P., Acceleration and loss of relativistic electrons during geomagnetic storms, *Geophys. Res. Lett.*, 2003, vol. 30, no. 10.
16. O'Brien, T.P., McPherron, R.L., Sornette, D., et al., Which magnetic storms produce relativistic electrons at

geosynchronous orbit?, *J. Geophys. Res.*, 2001, vol. 106, pp. 15533–15544.

17. Vlasova, N.A., Kovtyukh, A.S., Panasyuk, M.I., et al., Coupling between spatial, angular, and energetic distributions of particles on the geostationary orbit, *Kosm. Issled.*, 1989, vol. 27, no. 1, pp. 94–101.
18. Kovtyukh, A.S., On the form of the energetic spectrum of protons in the Earth's radiation belts and its formation mechanisms, *Geomagn. Aeron.*, 1985, vol. 25, no. 6, pp. 886–892.
19. Kovtyukh, A.S., Solar-cycle variations of invariant parameters of ion energy spectra of the Earth's radiation belts, *Cosmic Res.*, 1999, vol. 37, no. 1, pp. 53–64.
20. Kovtyukh, A.S., Panasyuk, M.I., Reizman, S.Ya., and Sosnovets, E.N., Spectral characteristics of protons on low and high altitudes during the geomagnetic storm of July 29, 1977, *Kosm. Issled.*, 1984, vol. 22, no. 3, pp. 399–405.
21. Kremser, G., Korth, A., Ullaland, S., et al., Energetic electron precipitation during a magnetospheric substorm and its relationship to wave particle interaction, *J. Geophys. Res.*, 1986, vol. 91, pp. 5711–5718.
22. Imhof, W.L. and Nightingale, R.W., Relativistic electron enhancements observed over a range of *L* shells trapped at high altitudes and precipitating at low altitudes into the atmosphere, *J. Geophys. Res.*, 1992, vol. 97, no. A5, pp. 6397–6403.
23. Kovtyukh, A.S., Coupling of pitch-angle and energetic distributions of ions in the Earth's radiation belts, *Geomagn. Aeron.*, 1993, vol. 33, no. 4, pp. 52–62.
24. Bashkirov, V.F. and Kovtyukh, A.S., Pitch-angle distributions of ions in the Earth's radiation belts: 3. Mathematical model for the real magnetic field, *Geomagn. Aeron.*, 1994, vol. 34, no. 2, pp. 29–37.
25. McIlwain, C.E., The radiation belts, natural and artificial, *Science*, 1963, vol. 142, pp. 355–361.
26. West, H.I., Jr. and Buck, R.M., Pitch angle distributions of energetic electrons in the equatorial regions of the outer magnetosphere—OGO-5 observations, in *Magnetospheric Physics*, McCormac, B.M., Ed., Dordrecht: D. Reidel, 1974, pp. 93–104.
27. Tverskoi, B.A., *Dinamika radiatsionnykh poyasov Zemli* (Dynamics of the Earth's Radiation Belts), Moscow: Nauka, 1968.
28. Hess, W.N., *The Radiation Belt and Magnetosphere*, Waltham, Massachusetts: Blaisdell, 1968.
29. Schulz, M. and Lanzerotti, L.J., *Particle Diffusion in the Radiation Belts*, New York: Springer, 1974.
30. Akasofu, S.-I. and Chapman, S., Solar–Terrestrial Physics, Oxford: Clarendon, 1972; Moscow: Mir, 1975.
31. Kovtyukh, A.S. and Panasyuk, M.I., The radiation belts of the Earth, in *Plazmennaya geliogeofizika* (Plasma Heliogeophysics), Zelenyi, L.M. and Veselovskii, I.S., Eds., Moscow: Fizmatlit, 2008, vol. 1, pp. 510–534.
32. Vlasova, N.A., Ginzburg, E.A., Kalegaev, V.V., et al., Penetration of solar cosmic rays into the Earth's magnetosphere on January 28, 2012, *Cosmic Res.*, 2013, vol. 51, no. 5, pp. 319–325.
33. Sadovnichy, V.A., Panasyuk, M.I., Bobrovnikov, S.Yu., et al., First results of investigating the space environment onboard the *Universitetskii-Tatyana* Satellite, *Cosmic Res.*, 2007, vol. 45, no. 4, pp. 273–387.
34. The Van Allen Probes Mission, *Space Sci. Rev.*, 2013, vol. 179, nos. 1–4.

Translated by N. Topchiev